Published in final edited form as:
J Cancer Ther Res. ; 2: 21–. doi:10.7243/2049-7962-2-21.

PCI-24781 (abexinostat), a novel histone deacetylase inhibitor, induces reactive oxygen species-dependent apoptosis and is synergistic with bortezomib in neuroblastoma

Giselle Saulnier Sholler[1], **Erika A. Currier**[2], **Akshita Dutta**[1], **Marni A. Slavik**[3], **Sharon A. Illenye**[4], **Maria Cecilia F. Mendonca**[5], **Julie Dragon**[3], **Stephen S. Roberts**[6], and **Jeffrey P. Bond**[3]

[1]Helen DeVos Children's Hospital/Michigan State University College of Medicine, Grand Rapids, MI

[2]Department of Pediatrics, University of Vermont College of Medicine, Burlington, VT

[3]Department of Microbiology and Molecular Genetics, University of Vermont College of Medicine, Burlington, VT

[4]Department of Research and Development, Haemtologic Technologies Inc., Essex Junction, VT

[5]Department of Pediatrics, Uniformed Services University of the Health Sciences, Bethesda, MD

[6]Department of Pediatrics Neuroblastoma Program, Memorial Sloan-Kettering Cancer Center, New York, NY

Abstract

In this study, we investigated the cytotoxic effects of a broad-spectrum histone deacetylase (HDAC) inhibitor, PCI-24781, alone and in combination with the proteasome inhibitor bortezomib in neuroblastoma cell lines. The combination was shown to induce synergistic cytotoxity involving the formation of reactive oxygen species. The cleavage of caspase-3 and PARP, as determined by western blotting, indicated that cell death was primarily due to apoptosis. Xenograft mouse models indicated increased survival among animals treated with this combination. The Notch signaling pathway and MYCN gene expression were quantified by reverse transcription-polymerase chain reaction (PCR) in cells treated with PCI-24781 and bortezomib, alone and in combination. Notch pathway expression increased in response to an HDAC inhibitor. NFKB1 and MYCN were both significantly down regulated. Our results suggest that PCI-24781 and bortezomib are synergistic in neuroblastoma cell lines and may be a new therapeutic strategy for this disease.

[*]**Corresponding Author:** Dr. Giselle Sholler, Helen DeVos Children's Hospital, 330 Barclay Ave., Grand Rapids, MI 49503 USA. Tel: (616) 267 0334; Giselle.SaulnierSholler@helendevoschildrens.org.

The authors disclose no potential conflicts of interest.

Author contributions

Conceived and designed the experiments: GSS, SSR, JPB. Performed the experiments: EAC, SAI, MFM, JD. Analysis and interpretation of the data: GSS, AD, MAS, JPB, SSR. Wrote the paper: MAS, AD, GSS, JPB, SSR.

Keywords

Neuroblastoma; apoptosis; PCI-24781 (abexinostat); bortezomib; ROS

Introduction

Neuroblastoma (NB) is the most common extracranial solid tumor in childhood, accounting for 12% of pediatric cancer fatalities annually in the United States (1). Despite advances in therapy, cure rates for Stage 4 high-risk neuroblastoma continue to be poor, with a five-year survival rate of only 30–40% in spite of intensive multimodality treatment (2). To date, no effective therapies exist for relapsed high-risk neuroblastoma, which remains uniformly fatal. The majority of cases of high risk neuroblastoma are initially sensitive to chemotherapy, but upon relapse they are inevitably highly chemoresistant (2,3). Novel treatments are therefore urgently needed (3).

Epigenetic regulation of gene transcription via histone deacetylation is an important mechanism in cellular homeostasis and has been implicated in tumorigenesis. Specifically, acetylation of the ε-amino group of lysine residues within the histone proteins maintains an open, transcriptionally active chromatin configuration (4,5). Histone deacetylases (HDACs) are a family of enzymes that remove these acetyl residues, allowing chromatin folding and resulting in inhibition of transcription. Additionally, HDACs have been found to modify the lysine residues of important non-histone proteins, including tumor suppressor p53 (6). Recent studies have shown that disruption of acetylation-deacetylation homeostasis may lead to the silencing of tumor suppressor pathways and may contribute to the development and progression of numerous malignancies (6–8).

HDAC inhibitors are a diverse class of compounds targeting those proteins that modulate transcription by removing acetyl groups from lysine residues in the histone tails of chromatin and by deacetylation of non-histone proteins. These compounds are actively being studied in numerous cancers (8–12). A potentially important effect of HDAC inhibitors is their induction of reactive oxygen species (ROS) including superoxide, leading to increased oxidative stress and apoptosis (13–16). HDAC inhibition produces growth inhibitory effects in NB cell lines *in vitro* (17, 18). First-generation HDAC inhibitors have had some clinical success to date, most notably vorinostat (suberoylanilide hydroxamic acid [SAHA]), which is approved by the FDA for use in cutaneous T-cell lymphoma (19). A phase I study of vorinostat with or without 13-*cis*-retinoic acid in refractory pediatric cancers (including NB) was recently completed and showed that SAHA was well-tolerated in children, the subset analysis for NB for safety was not reported (20). Despite their promise as novel anti-cancer agents, many first-generation HDAC inhibitors, including SAHA, have suffered from non-optimal pharmacokinetics and dosage regimens, leading to poor tolerance at therapeutic drug concentrations. This has led to a substantial effort to identify new, second-generation HDAC inhibitors having greater potency and specificity (21).

PCI-24781 (abexinostat; Pharmacyclics, Inc.) is a novel, second-generation phenyl hydroxamic acid–based, orally bioavailable HDAC inhibitor that has previously been shown

to have activity *in vitro* and *in vivo* against a broad array of cancers, including hematopoietic malignancies and bone and soft-tissue sarcomas (13, 22–24). It has also shown good tolerability and activity in Phase I and II clinical trials against lymphoma, as well as against solid tumors in Phase-I trials (25). Additionally, it acts as a potent radiosensitizing agent (26) and is synergistic with cytotoxic chemotherapy, such as doxorubicin (27) in preclinical models.

Bortezomib is a proteasome inhibitor currently used for first-line therapy of multiple myeloma and in relapsed mantle cell lymphoma (28). In both of these tumors, increased generation of ROS has been associated with cell death (29–31). Bortezomib was shown to induce apoptosis of NB cells as a single agent both in vitro and in vivo (32, 33).

Recently, Bhalla et al. showed that the combination of PCI-24781 plus bortezomib was synergistic and induced ROS-dependent apoptosis in Hodgkin and non-Hodgkin lymphoma cells (13). To our knowledge, however, there have been no reports of combining proteasome and HDAC inhibitors in NB. In this study, we show that the potent HDAC inhibitor PCI-24781 is both cytotoxic to NB cells as a single agent at nanomolar concentrations and is synergistic *in vitro* and *in vivo* with the proteasome inhibitor bortezomib. We also show that this combination therapy induces apoptosis, up-regulates Notch pathway signaling, and inhibits *MYCN* expression. These effects are abrogated by pretreatment with the antioxidant *N*-acetylcysteine, suggesting that ROS-mediated apoptosis induction may be a major mechanism of action.

Methods

Human neuroblastoma cell lines

The following NB cell lines were used in all experiments: SMS-KCNR, SKNBE(2)C, LA1-55n, and LAN2. The SMS-KCNR cell line was obtained from the lab of Dr. John Maris (Children's Hospital of Philadelphia, Philadelphia, PA). SKNBE(2)C, LA1-55n, and LAN2 cell lines were a gift from the labs of Drs. Robert Ross and Barbara Spengler (Fordham University, Bronx NY). All cell lines were authenticated using the Short Tandem Repeat method by the DNA Diagnostics Center (Fairfield, OH). All cell lines were cultured at 37 °C under humidified atmospheric oxygen and 5% CO_2 in RPMI 1640 (Mediatech, Manassas, VA) supplemented with 10% (v/v) FBS (Invitrogen, Carlsbad, CA), 100 units/mL penicillin, and 100 μg/mL streptomycin (Mediatech) as previously described (34–36).

Drugs and antibodies

The second-generation HDAC inhibitor PCI-24781 was provided by Pharmacyclics, Inc. (Sunnyvale, CA). Bortezomib and the HDAC inhibitor suberoylanilide hydroxamic acid (SAHA/vorinostat) were obtained from LC Laboratories (Woburn, MA). Sodium butyrate and valproic acid were from Sigma Aldrich (St. Louis, MO). Rabbit-anti-human cleaved-caspase-3 and mouse-anti-human PARP antibodies were purchased from Cell Signaling Technology (Danvers, MA).

Cell viability assays

Neuroblastoma cell lines were treated with various concentrations of bortezomib and PCI-24781(1–1000 nM) alone or in combination for 48 h. Cells were also treated with the HDAC inhibitors SAHA, sodium butyrate, and valproic acid. Cell viability was assessed using Calcein AM (AnaSpec, Freemont, CA). IC_{50} values for each compound or combination were calculated using Prism 5 software (GraphPad Inc., La Jolla, CA). Cell viability assays were repeated in the presence of 15 mM *N*-acetyl-L-cysteine (Sigma Aldrich, St. Louis, MO).

Measurements of fractional survival, *s*, at concentrations of bortezomib *b*, and PCI-24781 *p*, were interpreted with the aid of the model $s = \exp(\beta_{10}b + \beta_{01}p + \beta_{20}b^2 + \beta_{02}p^2 + \beta_{11}bp) + \varepsilon$, where β is the vector of model parameters and ε is the random error. Model parameters were estimated using the R software program (www.R-project.org).

Western blotting

Cells were treated for 48 h with HDAC inhibitors and/or bortezomib in 100-mm plates. Cells were collected by scraping, protein was extracted, and electrophoresis performed on a 15% SDS-polyacrylamide gel and blotted onto polyvinylidene fluoride (PVDF) membranes. The blots were probed with rabbit anti-human antibody to cleaved caspase 3 and β-actin, as well as mouse anti-human PARP antibody. Protein bands were visualized using infrared dye-conjugated anti-rabbit secondary antibodies (LI-COR Biosciences, Lincoln, NE) and photographed using an Odyssey Infrared Imaging System (LI-COR Biosciences).

mRNA preparation and gene expression profiling

SMS-KCNR cells were treated in duplicate with 4 nM bortezomib, 125 nM PCI-24781, or the combination for 24 h. RNA was extracted using the RNeasy micro kit (Qiagen, Valencia, CA) following the manufacturer's instructions and eluted in Riboblock RNase inhibitor (Formentas). RNA quality was verified with all calculated RIN scores above 9 (Quality control pass is RIN>6.5). Five micrograms of RNA per array was subsequently hybridized to Affymetrix GeneChip Human U133 Plus 2.0 arrays per the manufacturer's protocols. Arrays were analyzed by the Vermont Genetics Network Microarray Facility using Affymetrix GCOS software, according to the manufacturer's instructions. All other calculations were performed using R/BioConductor tools available from http://www.R-project.org. Probe set by sample matrix expression statistics were calculated using the Robust Multichip Average method (37, 38). Quality statistics were calculated using the Simpleaffy and affyQCReport packages (39).

Quantitative RT-PCR

Notch pathway and MYCN gene expression levels were measured using an Applied Biosystems 7500 Real-Time PCR system (Applied Biosystems, Foster City, CA) using dual-labeled fluorescent probes, with TaqMan One-Step RT-PCR Master Mix reagents (Applied Biosystems). Briefly, 50 or 100 ng of mRNA per reaction was used. Reaction conditions were 48 °C for 30 min, 95 °C for 10 min, followed by 95 °C for 15 s and 60 °C for 1 min, for a total of 40 cycles. Gene expression for *NOTCH1-4*, *JAG1* and *2*, *HES1*, and *MYCN*

was measured using TaqMan Assay-on-Demand predesigned probe sets (Applied Biosystems). The expression level of 18S ribosomal RNA was used as an endogenous control to normalize expression results, and fold changes between samples were calculated using the $2^{-\Delta\Delta Ct}$ method according to the manufacturer's instructions. Statistical analysis was performed using InStat Software (Graphpad).

In vivo assays

The Animal Care and Use Committee at the University of Vermont approved all animal studies. Six-week-old female nude mice (NCRNU-F, *CrTac:NCr-Foxn1^{nu}*) (Taconic Farms, Germantown, NY) were injected with 8×10^6 SMS-KCNR cells suspended in 0.2 mL of Matrigel subcutaneously into the left flank. Beginning 10 d post-injection, 6 mice per group were treated with daily intraperitoneal doses of vehicle control, 0.5 mg/kg bortezomib, 12.5 mg/kg PCI-24781, or a combination of bortezomib plus PCI-27481 at 0.5 and 12.5 mg/kg, respectively. Tumors were measured twice weekly and tumor volume was calculated using the ellipsoid formula [length x width x height x 0.52]. Treatment was continued until tumors exceeded 3.0 cm^3, at which point the mice were euthanized. Tumors were collected and weighed. The experiment was performed in duplicate.

Results

PCI-24781 and bortezomib exhibited single-agent cytotoxicity against NB cell lines

Four neuroblastoma cell lines SKNBE(2)C, SMS-KCNR, LA1-55n, and LAN2, were treated with various concentrations of four different HDAC inhibitors. Three of the inhibitors were first-generation drugs being tested in neuroblastoma clinical studies (SAHA, sodium butyrate, and valproic acid), and the fourth was the second-generation HDAC inhibitor PCI-24781 (Figure 1a). PCI-24781 exhibited the greatest cytotoxicity against the NB cell lines, with IC_{50} values ranging from 83.5 nM for SMS-KCNR to 196.4 nM for SKNBE(2)C. The IC_{50} values for the other HDAC inhibitors were for SAHA, 5.8–123.3 μM; for sodium butyrate, 3.8–10.4 mM; and for valproic acid, 2.0–17 mM. Bortezomib also exhibited cytotoxicity against the SMS-KCNR, LA1-55n and SKNBE(2)C cell lines (Figure 1b). The IC_{50} of bortezomib for these cell lines was estimated to be 2.4 nM for SMS-KCNR, 3.6 nM for LA1-55n, and 3.5 nM for SKNBE(2)C, but 37 μM for LAN2 cells.

PCI-24781 and bortezomib are synergistic

SMS-KNCR, LA1-55n, SKNBE(2)C, and LAN2 NB cell lines were treated with the combination of PCI-24781 plus bortezomib at various concentrations. Plots of cell survival as a function of the drug concentrations suggested that the two drugs act additively or synergistically over a wide range of concentrations. The contours of cell survival (solid lines) appear either straight or convex. Parameter estimation suggests synergism ($p = 0.01$). Closer inspection of one region of the PCI-24781/bortezomib dose plane with the LA1-55n cell line (Figure 1c) supports this conclusion. Consistent with synergism, PCI-24781 alone at up to 60 nM has no observable effect on survival, while it has a clear effect in the presence of 5 nM bortezomib.

PCI-24781 and bortezomib induced caspase-3-mediated apoptosis in NB cell lines

Treatment of neuroblastoma cell lines (SMS-KCNR and LA1-55n) with PCI-24781 and bortezomib agents led to induction of apoptosis as measured by the presence of cleaved PARP and of cleaved caspase-3 by western blotting (Figure 2). The amount of cleaved caspase-3 was greater after treatment with the combination of agents than with either agent alone.

N-acetyl-cysteine pretreatment blocked cytotoxicity of PCI-24781 and bortezomib

PCI-24781 induces the formation of reactive oxygen species in neuroblastoma cells. To confirm that the effect of these drugs involved the formation of ROS, cells were pretreated with the antioxidant *N*-acetyl-cysteine (NAC). Cells were then treated with either PCI-24781 (100 nM), bortezomib (6 nM), or both. In the absence of NAC, a decrease in cell viability was seen for the combination relative to the single agents (Figure 3). With 15 mM NAC pretreatment, the cytotoxicity of the combination was greatly decreased, indicating that the cytotoxicity induced by these agents involves ROS generation ($p<0.005$ based on 9 experiments representing a range of PCI-24781 and bortezomib concentrations, data not shown).

PCI-24781 and bortezomib up-regulated NOTCH pathway genes and suppressed *MYCN*

SMS-KCNR cells were treated with PCI-24781 (125nM), bortezomib (4nM), or the combination. After 24 h of treatment, microarray analysis revealed significant up-regulation of multiple various Notch signaling pathway genes (Table 1). The gene table was constructed using primary literature and Gene Ontology (GO, www.geneontology.org) termsfor notch signaling, oxidative stress and apoptosis. Genes differentially expressed between combination and control sample groups were identified based on at least 1.2 fold-change (in either direction) and adjusted p-value < 0.05 (Figure 4a, Table 1). Treatment with PCI-24781 alone resulted in up-regulation of *JAG1* at 6 h and up-regulation of *NOTCH2* at 24 h. These findings were confirmed using independent biological replicates by real-time qPCR (Figure 4b). Of importance in neuroblastoma, *MYCN* was suppressed with either bortezomib or PCI-24781 as well as with the combination at 24 h relative to controls.

PCI-24781 and bortezomib in combination increased survival in a mouse xenograft models

Nude [nu/nu] mice ($n = 6$) were injected with SMS-KCNR cells subcutaneously in the left flank. Once the tumors were palpable, the mice were treated once daily with vehicle, 0.5 mg/kg bortezomib, 12.5 mg/kg PCI-24781, or a combination of both. The tumors were measured twice weekly. Mice were euthanized when a maximum tumor size of 3 cm3 was reached. There were no signs of drug-related toxicities as noted by change in body weight or behavior. Neuroblastoma xenograft mice models showed an increase in time to survival from 55 days in the control group to 80 days in mice treated with the PCI-24781 plus bortezomib combination (Figure 6; $p = 0.001$).

Discussion

In this study, the HDAC inhibitor PCI-24781 had significant activity *in vitro* and *in vivo* as a single agent against several NB cell lines. Specifically, PCI-24781 showed dose-dependent

cytotoxicity with an IC_{50} of < 200 nM, which is well within previously reported clinically achievable range (40). This dose range was shown to have no cytotoxic effect on human normal foreskin fibroblast cell line HS-68 (41). This is in contrast to the other HDAC inhibitors tested (SAHA, sodium butyrate, and valproic acid), which had IC50 values in the micromolar to millimolar ranges. PCI-24781 induced apoptosis in all the NB cell lines tested, as shown by cleavage of caspase-3 and PARP. This effect was notably increased when combined with bortezomib. While PCI-24781 showed significant single-agent cytotoxicity, its synergy with bortezomib was striking. At doses that caused no effect as single agents, the combination of PCI-24781 plus bortezomib resulted in cell viability of 5% or less in all the cell lines tested. Treatment of mouse xenografts with this drug combination led to a doubling of mean survival time from 55 to 80 days. Importantly, the animals showed no evidence of systemic toxicity as reported by Bhalla et al as well (42), suggesting that this combination could be well tolerated in relapsed neuroblastoma patients, all of whom have been heavily pretreated with cytotoxic chemotherapy.

Gene expression profiling of NB cells treated with PCI-24781 plus bortezomib identified significant down-regulation of numerous genes, including *MYCN* and NFKB1. *MYCN* is a critically important proto-oncogene in NB, with nearly 1/3 of cases having *MYCN* amplification and associated poor outcomes (2). A report by Nawrocki et al. (43) showed that Myc regulates the sensitivity of multiple myeloma cells to bortezomib and SAHA-induced cell death. Interestingly, they found that the sensitivity of multiple myeloma to treatment with the combination of bortezomib and SAHA was increased in patients with overexpression of c-Myc. Our finding that treatment with PCI-24781 significantly down-regulated the expression of this critical neuroblastoma oncogene suggests that *MYCN*-amplified patients may particularly benefit from this therapy.

The mechanism by which HDAC inhibitors and bortezomib cause cell death remains controversial. Our results suggest that the observed cytotoxicity is ROS-dependent, as the effects of these compounds (especially in combination) were significantly decreased when cells were pretreated with the antioxidant NAC. Both PCI-24781 and bortezomib have been shown independently to cause ROS generation; additionally, PCI-24781 was previously shown to suppress NF-KB expression, a critically important regulator of the cellular oxidative stress response (13). Our findings confirm these observations. It seems plausible that the combination of these two compounds leads to both increased ROS generation and suppression of important oxidative stress responses, leading to increased apoptosis.

Interestingly, our gene expression studies identified the Notch signaling pathway as a significantly up-regulated pathway in our cell lines after treatment with PCI-24781 plus bortezomib. While it is well established that Notch genes function as oncogenes in hematologic malignancies, most notable T-cell acute lymphoblastic leukemia, its specific role remains controversial in solid tumors (44). Notch signaling has been shown to be oncogenic in breast and colon cancers among others (45, 46), but it acts as a tumor suppressor in skin and pancreatic cancer models (47, 48).

Two previous studies of HDAC inhibitors in neuroblastoma showed up-regulation of the Notch pathway in response to HDAC inhibitor treatment (49, 50). They also showed that

this treatment up-regulated genes known to be involved in cellular differentiation and growth arrest, leading them to hypothesize that increased Notch signaling was exerting a tumor suppressor effect. On the other hand, more recent studies in neuroblastoma have suggested that increased levels of Notch pathway gene expression correlate with advanced stages and worse clinical outcome, and that blockade of Notch signaling inhibits neuroblastoma growth *in vitro* and *in vivo* (51, 52). These seemingly contradictory roles of Notch signaling suggest that its effects are likely highly dependent on cellular context and on interactions with other signaling pathways and the tumor microenvironment. This has clearly been shown to be true for many other solid tumors (44). Additional studies are needed to draw conclusions regarding the role of Notch signaling in neuroblastoma.

In summary, our results show that the HDAC inhibitor PCI-24781, when given as a single agent, exhibited significant cytotoxicity and induced apoptosis in a panel of NB cell lines. The combination of PCI-24781 and bortezomib was strongly synergistic in cell lines tested and significantly prolonged survival in xenograft models compared to either agent alone. This anti-NB activity appears to be ROS-dependent, as shown by prevention of apoptosis and cell death with NAC pretreatment. Enhanced generation of ROS combined with simultaneous inhibition of oxidative stress response genes may represent an important mechanism underlying NB cell death caused by this drug combination. Our finding of significantly decreased expression of NF-KB, one of the primary regulators of oxidative stress response in cells, supports this hypothesis. Finally, we showed that treatment with this combination led to significant up-regulation of many members of the Notch signaling pathway, suggesting a novel pathway of action of these compounds in neuroblastoma that deserves further study. These data suggest that PCI-24781 has a potential for use in the treatment of neuroblastoma, both alone and in combination with bortezomib, and future clinical trials in NB patients using these agents should be explored.

Acknowledgements

This work was supported by the Friends of Will/Beat NB Foundation, Max’s Ring of Fire, Owen Moscone Foundation, and Charles and Meryl Witmer Foundation and donations from many families and supporters of neuroblastoma research. We thank Scott Tighe of the Vermont Genetics Network. This publication was made possible by the Vermont Genetics Network through Grant no. P20 RR16462 from INBRE Program of the National Center for Research Resources (NCRR), a component of National Institutes of Health (NIH). Its contents are solely the responsibility of the authors and do not necessarily represent the official views of NCRR and NIH. We thank Dr. Sriram Balasubramanian (Pharmacyclics, Inc.) for providing PCI-24781.

References

1. Smith MA, Seibel NL, Altekruse SF, Ries LA, Melbert DL, O'Leary M, et al. Outcomes for children and adolescents with cancer: challenges for the twenty-first Century. J Clin Oncol. 2010; 28:2625–2634. [PubMed: 20404250]
2. Maris JM, Hogarty MD, Bagatell R, Cohn SL. Neuroblastoma. Lancet. 2007; 369:2106–2120. [PubMed: 17586306]
3. Maris JM. Recent advances in neuroblastoma. N Engl J Med. 2010; 362:2202–2211. [PubMed: 20558371]
4. Dokmanovic M, Clarke C, Marks PA. Histone deacetylase inhibitors: overview and perspectives. Mol Cancer Res. 2007; 5:981–989. [PubMed: 17951399]
5. Xu WS, Parmigiani RB, Marks PA. Histone deacetylase inhibitors: molecular mechanisms of action. Oncogene. 2007; 26:5541–5552. [PubMed: 17694093]

6. Buchwald M, Kramer OH, Heinzel T. HDACi--targets beyond chromatin. Cancer Lett. 2009; 280:160–167. [PubMed: 19342155]

7. Richon VM, O'Brien JP. Histone deacetylase inhibitors: a new class of potential therapeutic agents for cancer treatment. Clin Cancer Res. 2002; 8:662–664. [PubMed: 11895892]

8. Minucci S, Pelicci PG. Histone deacetylase inhibitors and the promise of epigenetic [and more] treatments for cancer. Nat Rev Cancer. 2006; 6:38–51. [PubMed: 16397526]

9. Sakuma T, Uzawa K, Onda T, Shiiba M, Yokoe H, Shibahara T, Tanzawa H. Aberrant expression of histone deacetylase 6 in oral squamous cell carcinoma. Int J Oncol. 2006; 29:117–124. [PubMed: 16773191]

10. Wilson AJ, Byun DS, Popova N, Murray LB, L'Italien K, Sowa Y, Arango D, Velcich A, Augenlicht LH, Mariadason JM. Histone deacetylase 3 [HDAC3] and other class I HDACs regulate colon cell maturation and p21 expression and are deregulated in human colon cancer. J Biol Chem. 2006; 281:13548–13558. [PubMed: 16533812]

11. Kim HR, Kim EJ, Yang SH, Jeong ET, Park C, Lee JH, Youn MJ, So HS, Park R. Trichostatin A induces apoptosis in lung cancer cells via simultaneous activation of the death receptor-mediated and mitochondrial pathway? Exp Mol Med. 2006; 38:616–624. [PubMed: 17202837]

12. Qu W, Kang YD, Zhou MS, Fu LL, Hua ZH, Wang LM. Experimental study on inhibitory effects of histone deacetylase inhibitor MS-275 and TSA on bladder cancer cells. Urol Oncol. 2009; 28:648–654. [PubMed: 19181544]

13. Bhalla S, Balasubramanian S, David K, Sirisawad M, Buggy J, Mauro L, Prachand S, Miller R, Gordon LI, Evens AM. PCI-24781 induces caspase and reactive oxygen species-dependent apoptosis through NF-kappaB mechanisms and is synergistic with bortezomib in lymphoma cells. Clin Cancer Res. 2009; 15:3354–3365. [PubMed: 19417023]

14. Ungerstedt JS, Sowa Y, Xu WS, Shao Y, Dokmanovic M, Perez G, Ngo L, Holmgren A, Jiang X, Marks PA. Role of thioredoxin in the response of normal and transformed cells to histone deacetylase inhibitors. Proc Natl Acad Sci U S A. 2005; 102:673–678. [PubMed: 15637150]

15. Ruefli AA, Ausserlechner MJ, Bernhard D, Sutton VR, Tainton KM, Kofler R, Smyth MJ, Johnstone RW. The histone deacetylase inhibitor and chemotherapeutic agent suberoylanilide hydroxamic acid [SAHA] induces a cell-death pathway characterized by cleavage of Bid and production of reactive oxygen species. Proc Natl Acad Sci U S A. 2001; 98:10833–10838. [PubMed: 11535817]

16. Xu W, Ngo L, Perez G, Dokmanovic M, Marks PA. Intrinsic apoptotic and thioredoxin pathways in human prostate cancer cell response to histone deacetylase inhibitor. Proc Natl Acad Sci U S A. 2006; 103:15540–15545. [PubMed: 17030815]

17. Oehme I, Deubzer HE, Wegener D, Pickert D, Linke JP, Hero B, Kopp-Schneider A, Westermann F, Ulrich SM, Deimling AV, Fischer M, Witt O. Histone deacetylase 8 in neuroblastoma tumorigenesis. Clin Cancer Res. 2009; 15:91–99. [PubMed: 19118036]

18. De los Santos M, Zambrano A, Aranda A. Combined effects of retinoic acid and histone deacetylase inhibitors on human neuroblastoma SH-SY5Y cells. Mol Cancer Ther. 2007; 6:1425–17432. [PubMed: 17431121]

19. Richon VM, Garcia-Vargas J, Hardwick JS. Development of vorinostat: current applications and future perspectives for cancer therapy. Cancer Lett. 2009; 280:201–210. [PubMed: 19181442]

20. Fouladi M, Park JR, Stewart CF, Gilbertson RJ, Schaiquevich P, Sun J, Reid JM, Ames MM, Roseanne S, Ingle AM, Zwiebel J, Blaney SM, et al. Pediatric phase I trial and pharmacokinetic study of vorinostat: a Children's Oncology Group phase I consortium report. J Clin Oncol. 2010; 28:3623–3629. [PubMed: 20606092]

21. Ganesan A, Nolan L, Crabb SJ, Packham G. Epigenetic therapy: histone acetylation, DNA methylation and anti-cancer drug discovery. Curr Cancer Drug Targets. 2009; 9:963–981. [PubMed: 20025605]

22. Rivera-Del Valle N, Gao S, Miller CP, Fulbright J, Gonzales C, Sirisawad M, Steggerda S, Wheler J, Balasubramanian S, Chandra J. PCI-24781, a Novel Hydroxamic Acid HDAC Inhibitor, Exerts Cytotoxicity and Histone Alterations via Caspase-8 and FADD in Leukemia Cells. Int J Cell Biol. 2010; 2010:207420. [PubMed: 20145726]

23. Yang C, Choy E, Hornicek FJ, Wood KB, Schwab JH, Liu X, Mankin H, Duan Z. Histone deacetylase inhibitor [HDACI] PCI-24781 potentiates cytotoxic effects of doxorubicin in bone sarcoma cells. Cancer Chemother Pharmacol. 2011; 67(2):439–446. [PubMed: 20461381]
24. Lopez G, Liu J, Ren W, Wei W, Wang S, Lahat G, Zhu QS, Bornmann WG, McConkey DJ, Pollock RE, Lev DC. Combining PCI-24781, a novel histone deacetylase inhibitor, with chemotherapy for the treatment of soft tissue sarcoma. Clin Cancer Res. 2009; 15:3472–3483. [PubMed: 19417021]
25. Undevia LS, Schilsky R, Loury D, Balasubramanian S, Mani C, Sirisawad M, Buggy JJ, Miller RA, Ratain MJ. Phase I study of the safety, pharmacokinetics [PK] and pharmacodynamics [PD] of the histone deacetylase inhibitor [HDACi] PCI-24781. J Clin Oncol. 2008 May.20:14514.
26. Banuelos CA, Banath JP, MacPhail SH, Zhao J, Reitsema T, Olive PL. Radiosensitization by the histone deacetylase inhibitor PCI-24781. Clin Cancer Res. 2007; 13:6816–6826. [PubMed: 18006784]
27. Yang C, Choy E, Hornicek FJ, Wood KB, Schwab JH, Liu X, Mankin H, Duan Z. Histone deacetylase inhibitor (HDACI) PCI-24781 potentiates cytotoxic effects of doxorubicin in bone sarcoma cells. Cancer Chemother Pharmacol. 2011 Feb; 67(2):439–446. Perez-Galan P, Roue G. [PubMed: 20461381]
28. Richardson PG, Barlogie B, Berenson J, Singhal S, Jagannath S, Irwin D, Rajkumar SV, Srkalovic G, Alsina M, Alexanian R, Siegel D, Orlowski RZ, Kuter D, Limentani SA, Lee S, Hideshima T, Esseltine DL, Kauffman M, Adams J, Schenkein DP, Anderson KC. A phase 2 study of bortezomib in relapsed, refractory myeloma. N Engl J Med. 2003 Jun 26; 348(26):2609–2617. [PubMed: 12826635]
29. Villamor N, Montserrat E, Campo E, Colomer D. The proteasome inhibitor bortezomib induces apoptosis in mantle-cell lymphoma through generation of ROS and Noxa activation independent of p53 status. Blood. 2006; 107:257–264. [PubMed: 16166592]
30. Yu C, Rahmani M, Dent P, Grant S. The hierarchical relationship between MAPK signaling and ROS generation in human leukemia cells undergoing apoptosis in response to the proteasome inhibitor Bortezomib. Exp Cell Res. 2004; 295:555–566. [PubMed: 15093752]
31. Ling YH, Liebes L, Zou Y, Perez-Soler R. Reactive oxygen species generation and mitochondrial dysfunction in the apoptotic response to Bortezomib, a novel proteasome inhibitor, in human H460 non-small cell lung cancer cells. J Biol Chem. 2003; 278:33714–33723. [PubMed: 12821677]
32. Valentiner U, Haane C, Nehmann N, Schumacher U. Effects of bortezomib on human neuroblastoma cells in vitro and in a metastatic xenograft model. Anticancer Res. 2009; 29:1219–1225. [PubMed: 19414367]
33. Armstrong MB, Schumacher KR, Mody R, Yanik GA, Opipari AW Jr, Castle VP. Bortezomib as a therapeutic candidate for neuroblastoma. J Exp Ther Oncol. 2008; 7:135–145. [PubMed: 18771087]
34. Rettig WJ, Spengler BA, Chesa PG, Old LJ, Biedler JL. Coordinate changes in neuronal phenotype and surface antigen expression in human neuroblastoma cell variants. Cancer Res. 1987; 47:1383–1389. [PubMed: 3028608]
35. Reynolds CP, Tomayko MM, Donner L, Helson L, Seeger RC, Triche TJ, Brodeur GM. Biological classification of cell lines derived from human extra-cranial neural tumors. Prog Clin Biol Res. 1988; 271:291–306. [PubMed: 3406003]
36. Walton, JD.; Kattan, DR.; Thomas, SK.; Spengler, BA.; Guo, HF.; Biedler, JL.; Cheung, NKV.; Ross, RR. Neoplasia. Vol. 6. New York, NY: 2004. Characteristics of stem cells from human neuroblastoma cell lines and in tumors; p. 838-845.
37. Irizarry RA, Bolstad BM, Collin F, Cope LM, Hobbs B, Speed TP. Summaries of Affymetrix GeneChip probe level data. Nucleic Acids Res. 2003; 31:e15. [PubMed: 12582260]
38. Bolstad BM, Irizarry RA, Astrand M, Speed TP. A comparison of normalization methods for high density oligonucleotide array data based on variance and bias. Bioinformatics. 2003; 19:185–193. [PubMed: 12538238]
39. Wilson CL, Miller CJ. Simpleaffy: a BioConductor package for Affymetrix Quality Control and data analysis. Bioinformatics. 2005; 21:3683–3685. [PubMed: 16076888]

40. Adimoolam S, Sirisawad M, Chen J, Thiemann P, Ford JM, Buggy JJ. HDAC inhibitor PCI-24781 decreases RAD51 expression and inhibits homologous recombination. Proc Natl Acad Sci U S A. 2007; 104:19482–19487. [PubMed: 18042714]
41. Zhan Q, Tsai S, Lu Y, Wang C, Kwan Y, et al. RuvBL2 Is Involved in Histone Deacetylase Inhibitor PCI-24781-Induced Cell Death in SK-N-DZ Neuroblastoma Cells. PLoS ONE. 2013; 8(8):e71663. [PubMed: 23977108]
42. Bhalla S, Balasubramanian S, David K, Sirisawad M, Buggy J, Mauro L, Prachand S, Miller R, Gordon L, Evens A. The Histone Deacetylase Inhibitor PCI-24781 Induces Caspase and ROS-Dependent Apoptosis Through NF-KB and is Synergistic with Bortezomib in Lymphoma Cells. Clin Cancer Res. 2009 May 15; 15(10):3354–3365. [PubMed: 19417023]
43. Nawrocki ST, Carew JS, Maclean KH, Courage JF, Huang P, Houghton JA, Cleveland JL, Giles FJ, McConkey DJ. Myc regulates aggresome formation, the induction of Noxa, and apoptosis in response to the combination of bortezomib and SAHA. Blood. 2008; 112:2917–2926. [PubMed: 18641367]
44. Ranganathan P, Weaver KL, Capobianco AJ. Notch signalling in solid tumours: a little bit of everything but not all the time. Nat Rev Cancer. 2011; 11:338–351. [PubMed: 21508972]
45. Reedijk M, Odorcic S, Chang L, Zhang H, Miller N, McCready DR, Lockwood G, Egan SE. High-level coexpression of JAG1 and NOTCH1 is observed in human breast cancer and is associated with poor overall survival. Cancer Res. 2005; 65:8530–8537. [PubMed: 16166334]
46. Zhang Y, Li B, Ji ZZ, Zheng PS. Notch1 regulates the growth of human colon cancers. Cancer. 2010; 116:5207–5218. [PubMed: 20665495]
47. Hanlon L, Avila JL, Demarest RM, Troutman S, Allen M, Ratti F, Rustgi AK, Stanger BZ, Radtke F, Adsay V, Long F, Capobianco AJ, et al. Notch1 functions as a tumor suppressor in a model of K-ras-induced pancreatic ductal adenocarcinoma. Cancer Res. 2010; 70:4280–4286. [PubMed: 20484026]
48. Nicolas M, Wolfer A, Raj K, Kummer JA, Mill P, van Noort M, Hui CC, Clevers H, Dotto GP, Radtke F. Notch1 functions as a tumor suppressor in mouse skin. Nat Genet. 2003; 33:416–421. [PubMed: 12590261]
49. Stockhausen MT, Sjolund J, Manetopoulos C, Axelson H. Effects of the histone deacetylase inhibitor valproic acid on Notch signalling in human neuroblastoma cells. Br J Cancer. 2005; 92:751–759. [PubMed: 15685243]
50. de Ruijter AJ, Meinsma RJ, Bosma P, Kemp S, Caron HN, van Kuilenburg AB. Gene expression profiling in response to the histone deacetylase inhibitor BL1521 in neuroblastoma. Exp Cell Res. 2005; 309:451–467. [PubMed: 16084510]
51. Ferrari-Toninelli G, Bonini SA, Uberti D, Buizza L, Bettinsoli P, Poliani PL, Facchetti F, Memo M. Targeting Notch pathway induces growth inhibition and differentiation of neuroblastoma cells. Neuro Oncol. 2010; 12:1231–1243. [PubMed: 20716592]
52. Chang HH, Lee H, Hu MK, Tsao PN, Juan HF, Huang MC, Shih YY, Wang BJ, Jeng YM, Chang CL, Huang SF, Tsay YG, et al. Notch1 expression predicts an unfavorable prognosis and serves as a therapeutic target of patients with neuroblastoma. Clin Cancer Res. 2010; 16:4411–4420. [PubMed: 20736329]

A

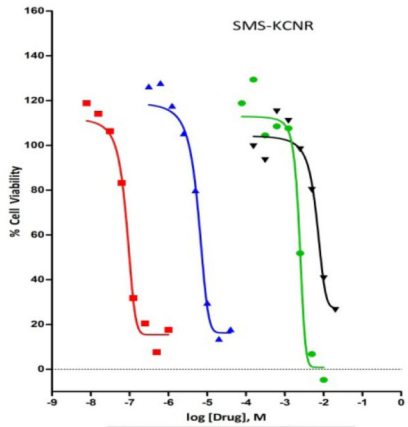

Drug	IC_{50}	F. P.
PCI-24781	83.5nM	
SAHA	5.83uM	-70X
Sodium Butyrate	6.62mM	-79,281X
Valproic Acid	2.42mM	-28,982X

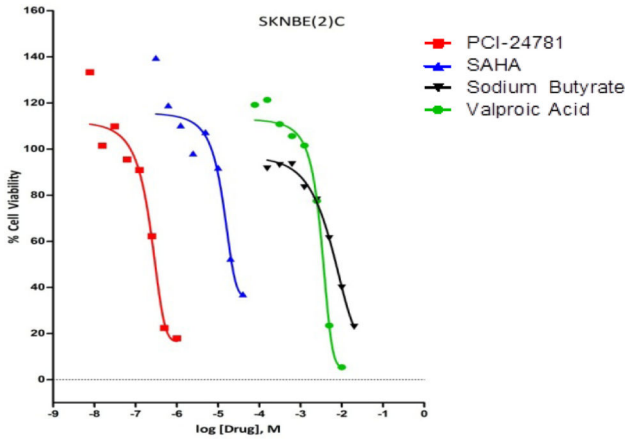

Drug	IC_{50}	F. P.
PCI-24781	196.4 nM	—
SAHA	12.3 μM	−63X
Sodium Butyrate	10.4 mM	−52,953X
Valproic Acid	3.1 mM	−15,748X

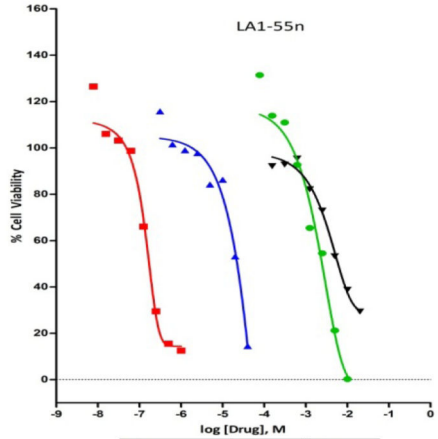

Drug	IC_{50}	F. P.
PCI-24781	122.6 nM	
SAHA	123.3 uM	−1,006X
Sodium Butyrate	5.3 mM	−43,230X
Valproic Acid	17.4 mM	−141,925X

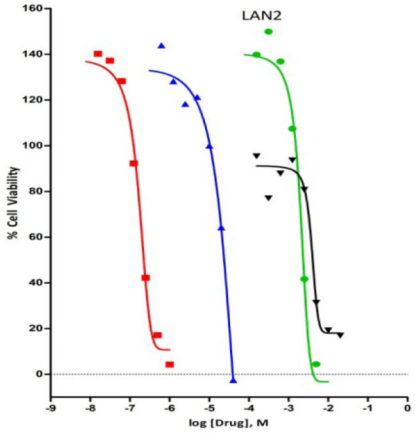

Drug	IC_{50}	F. P.
PCI-24781	163.1 nM	—
SAHA	18.4 μM	−113X
Sodium Butyrate	3.8 mM	−23,299X
Valproic Acid	2.0 mM	−12,262X

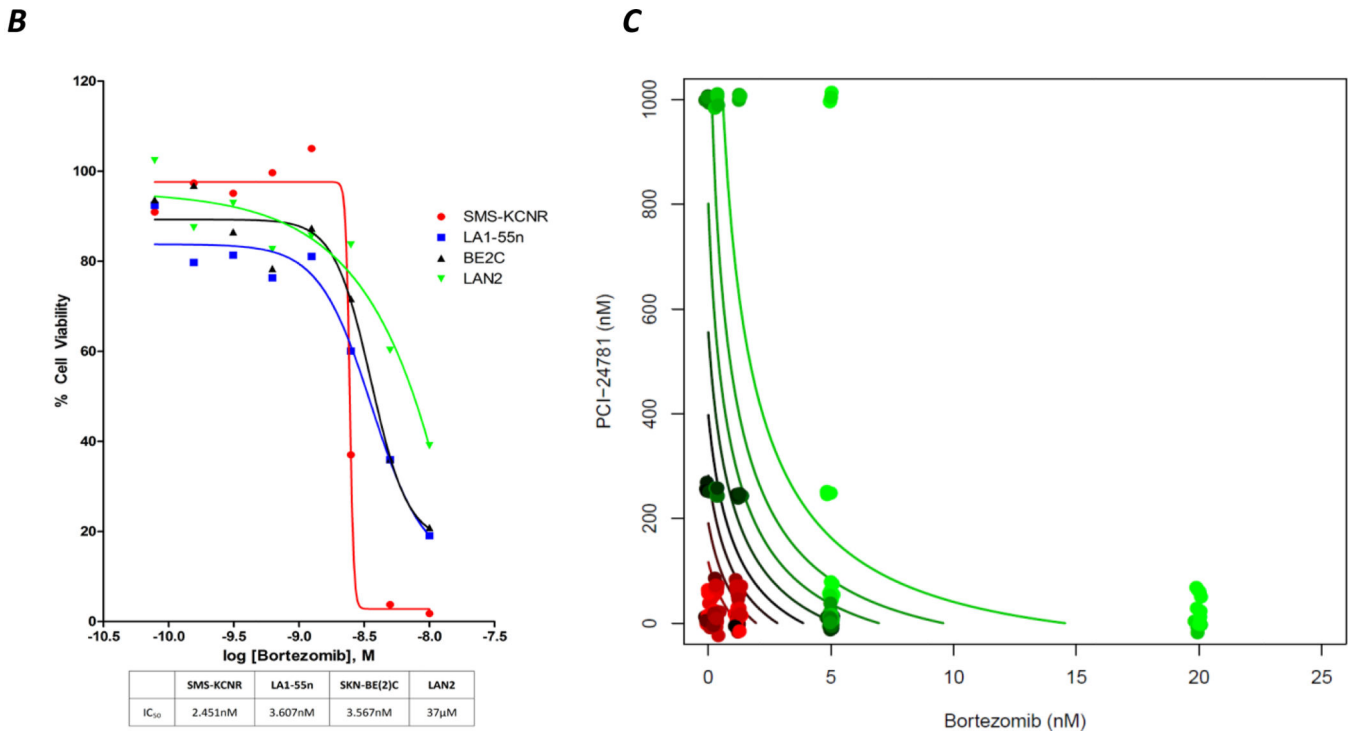

	SMS-KCNR	LA1-55n	SKN-BE(2)C	LAN2
IC_{50}	2.451nM	3.607nM	3.567nM	37μM

Figure 1. PCI-24781 is a more potent inhibitor of cell viability than other HDAC inhibitors and synergizes with bortezomib

(A) IC50 values of HDAC Inhibitors (PCI-24781, SAHA, valproic acid and sodium butyrate) were established in four NB cell lines. Cells were treated with increasing drug concentrations for 48 hrs followed by cell viability assay.

(b) IC50 value of bortezomib was established in four NB cell lines. Cell lines were treated with Bortezomib for 48 hrs, with increasing concentrations followed by cell viability assay

(c) Isobologram showing that the combination of PCI-24781 plus bortezomib is synergistic for the LA1-55n cell line. Points express mean survival after treatment with one or both drugs. Survival is expressed by the points' color, ranging from 100% survival (red) through 50% (black) to 0% (green). Contours represent the predictions obtained by fitting the model to data. Contour lines are colored according to percent survival, the curvature reflects synergism.

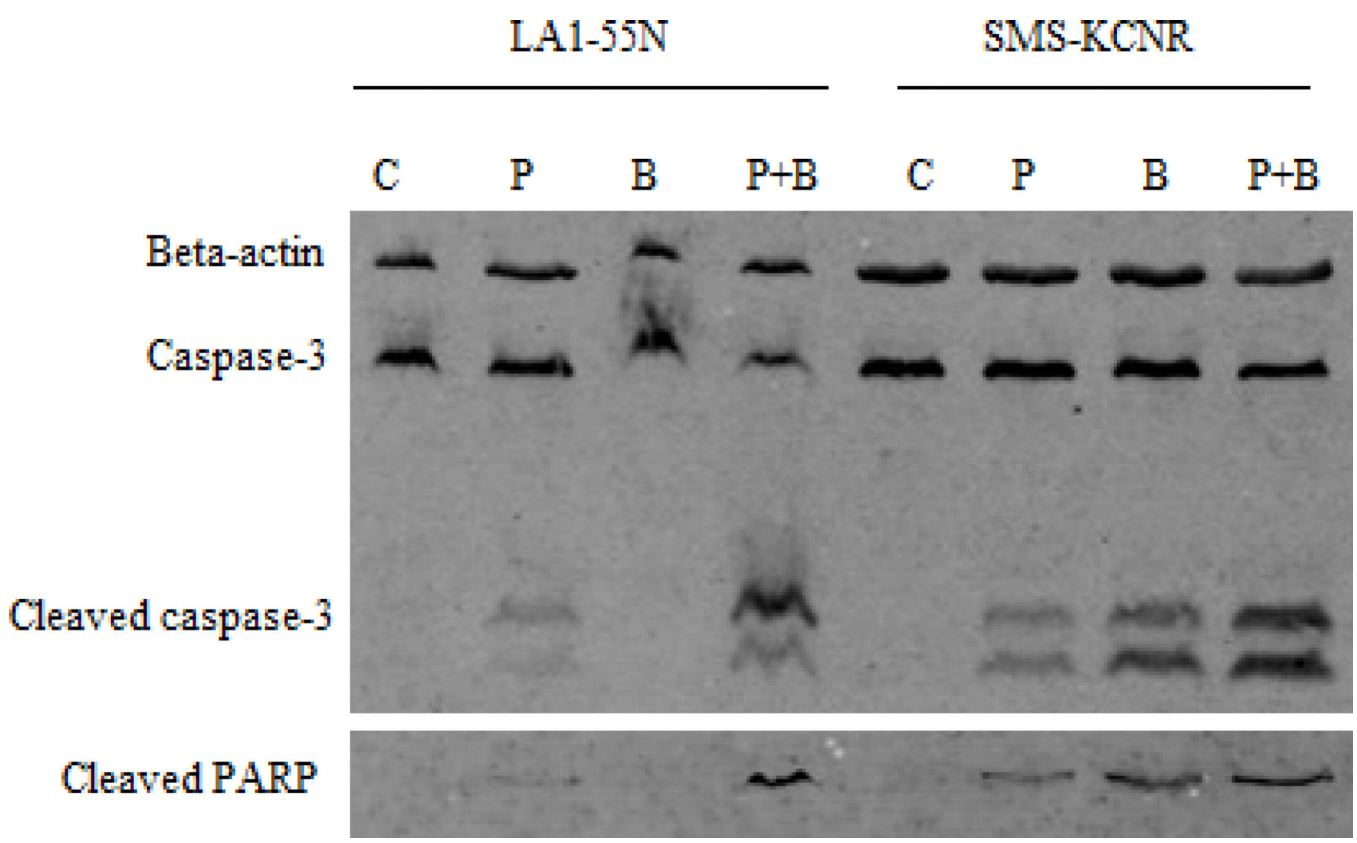

Figure 2. Treatment with PCI-24781 and bortezomib result in caspase mediated apoptosis in neuroblastoma

Cells were incubated with vehicle (C), 1 μM PCI-24781 (P), 10 mM bortezomib (B), or the combination (P+B) for 48 hrs and cell lysates were collected and run on western blots to evaluate for cleaved caspase 3 and PARP.

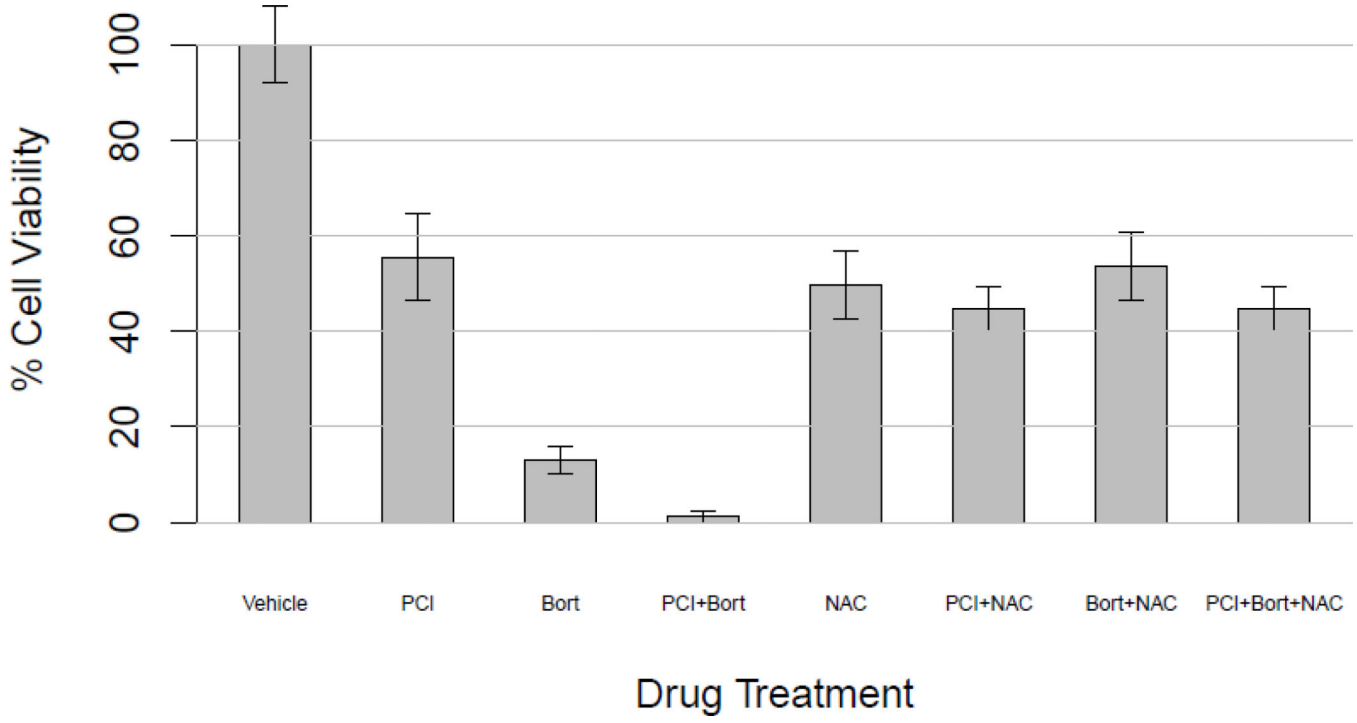

Figure 3. N-acetyl-cysteine pretreatment blocks cytotoxicity of PCI-24781 plus bortezomib

Cells were pre-incubated with 15 mM NAC or vehicle (control), and then treated with 100 nM PCI-24781, 6 nM bortezomib, or both and incubated for 48 hours followed by cell viability assay (p value <0.005).

a

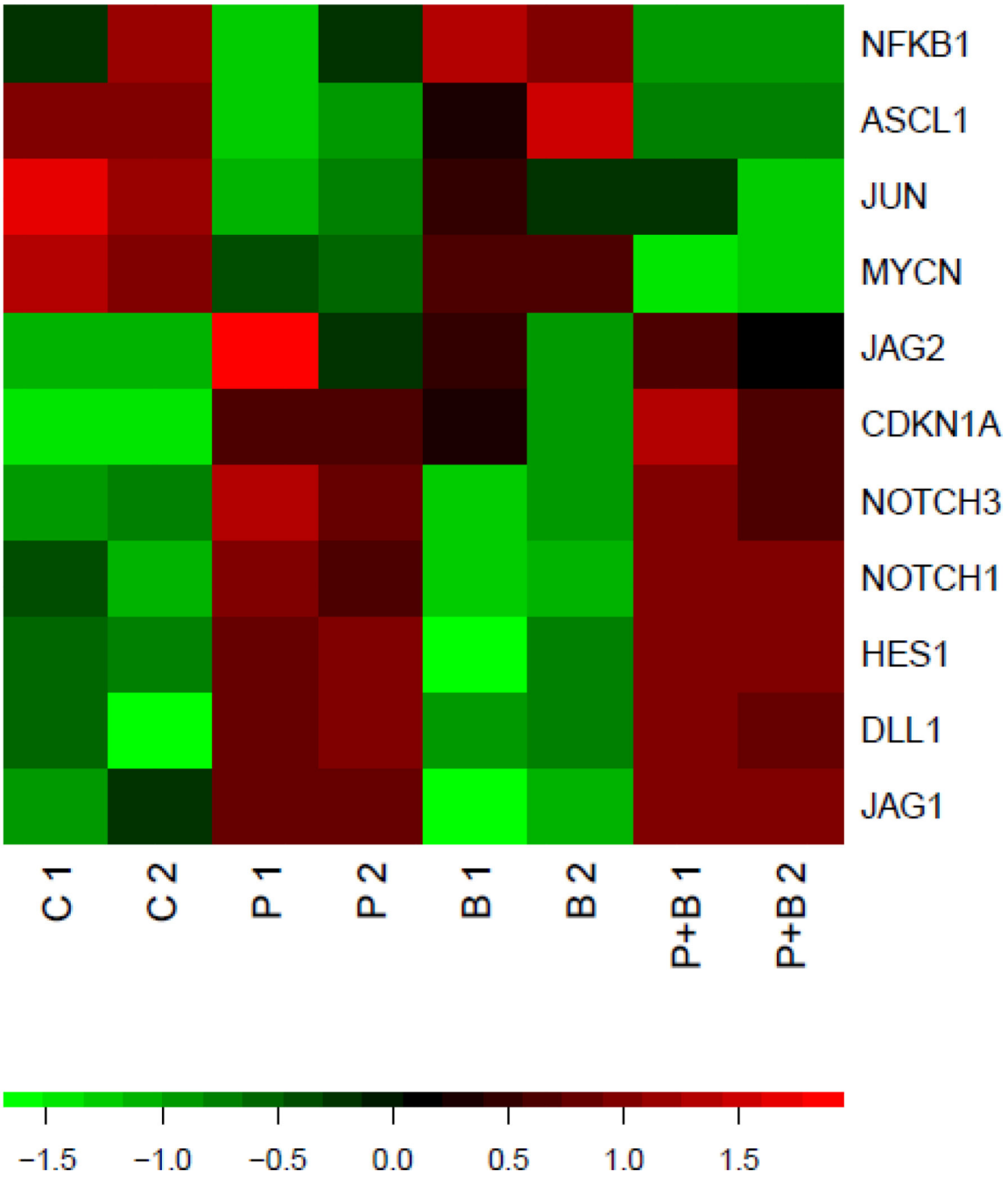

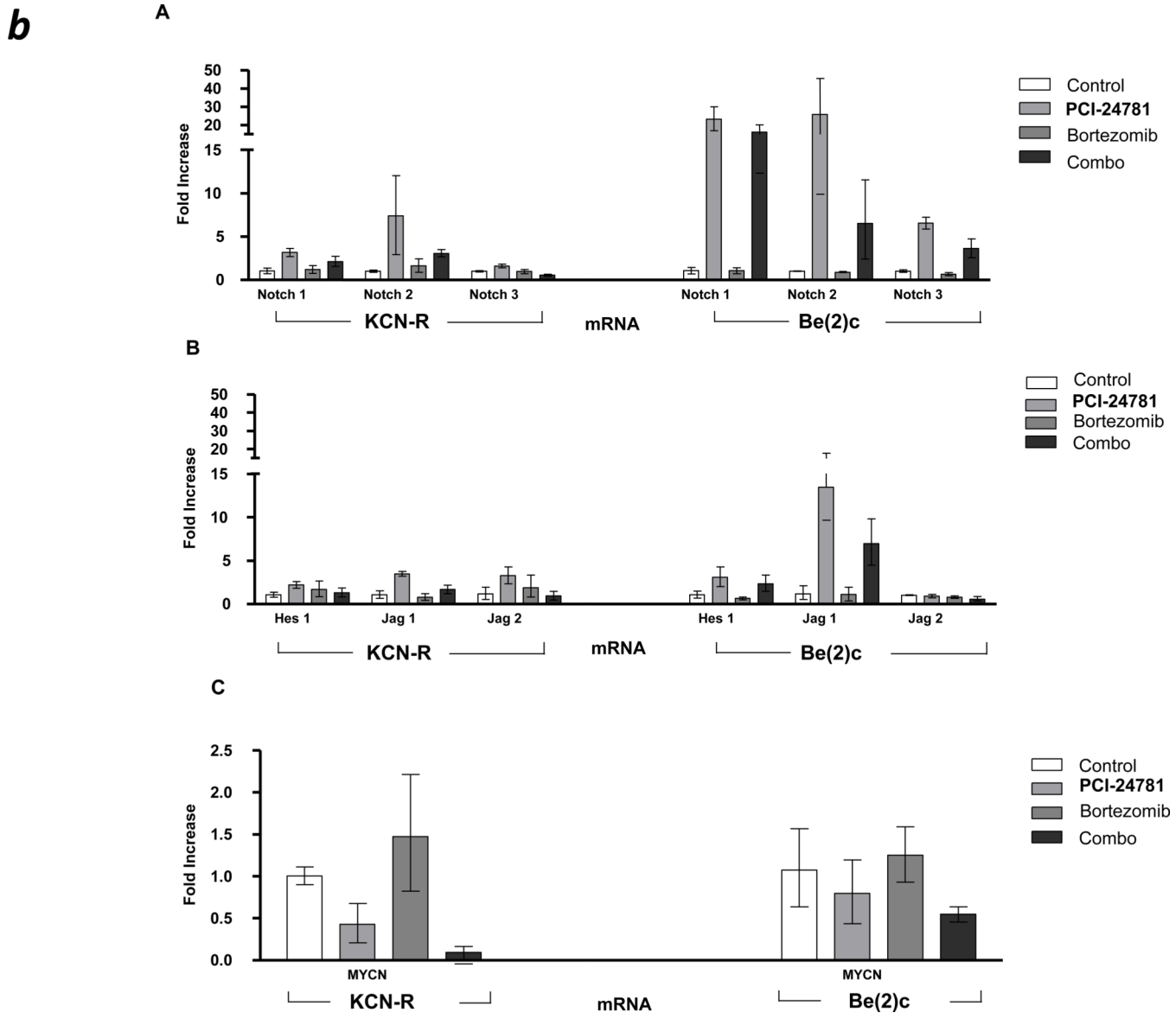

Figure 4. PCI-24781 treatment up-regulates NOTCH pathway genes and suppresses MYCN, as confirmed by RT-PCR

(a) SMS-KCNR cells were treated in duplicate with 4 nM bortezomib, 125 nM PCI-24781, or the combination for 24 h. RNA was isolated and hybridized to Affymetrix U133 2+ arrays. Rows represent genes; columns represent samples. P 1 and P 2 represent replicate PCI-24781 treatments; B 1 and B 2 represent Bortezomib treatments; P+B 1 and P+B 2 represent PCI-24781 in combination with Bortezomib. The color represents elevated (red) or diminished (green) expression relative to the mean value for the gene and standardized. Rows were ordered to emphasize distinct expression patterns. (b) Real-time PCR for Notch genes confirmed up regulation of expression seen in microarrays in SMS KCNR cells. (A) Notch expression after treatment with PCI-24781 alone and in combination with bortezomib was statistically significantly increased ($P<0.05$) in each case except for Notch 3 in SMS-KCNR cells (P=n.s.). Notch 4 was not expressed in any of the cell lines tested. (B)

PCI-24781 treatment significantly up regulated expression of the HES1 in both cell lines ($P<0.05$). JAG1 and JAG2 were both significantly up regulated by PCI-24781 in SMS-KCNR cells ($P<0.01$) but JAG2 was not significantly changed in SKNBE(2)C cells. (C) MCYN expression was significantly decreased by treatment with PCI-24781 along and in combination with bortezomib in both cell lines ($P<0.01$), while treatment with bortezomib alone did not significantly change MYCN expression (P=n.s.)

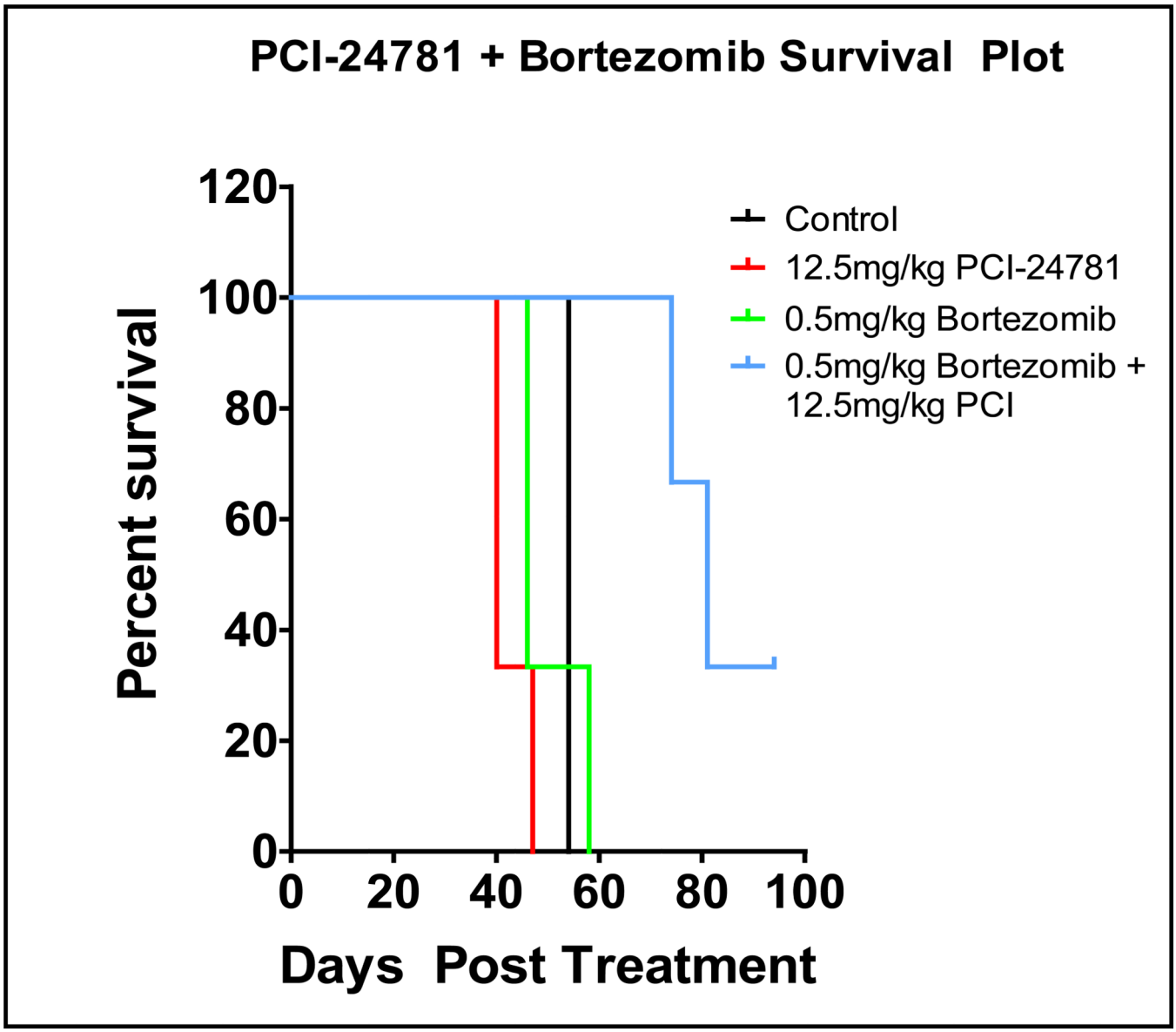

Figure 5. PCI-2471 and bortezomib increased survival in vivo in a neuroblastoma mouse SMSKCNR xenograft model

Mice were treated daily with either vehicle control, 12.5 mg/kg PCI-2471 IP, 0.5mg/kg bortezomib IP or combination until tumors reached a maximum volume of $3cm^3$ (survival end point, $p = 0.001$).

Table 1

Genes of SMS-KCNR cells in five categories differentially expressed upon 24-h treatment with PCI-24781, bortezomib and both

Up-regulated genes are shown as positive fold change values and down-regulated genes are shown as negative fold change values.

		PBmC		PmC		BmC	
Accn #	**Gene Title/Gene Symbol**	**F.C.**	**P-value**	**F.C.**	**P-value**	**F.C.**	**P-value**
Notch Signaling Pathway							
NM_004316	Achaete-scute complex homolog 1 *(ASCL1)*	**−3.002**	0.000927	−3.86901	0.00017	−2.19856	0.231699
NM_000389	Cyclin-dependent kinase inhibitor 1A *(CDKN1A)*	**−2.60325**	0.002993	−2.71053	1.31E-05	−1.39463	0.478301
NM_005618	Delta-like 1 *(DLL1)*	3.033902	0.024784	2.877812	0.002491	1.256778	0.790808
NM_005524	Hairy and enhancer of split 1 *(HES1)*	2.205546	0.001785	2.215463	2.96E-05	1.076456	0.895074
NM_012259	Hairy/enhancer-of-split related with YRPW motif 2 *(HEY2)*	1.394142	0.081298	1.391811	0.010457	−1.01637	0.998356
NM_000214	Jagged 1 *(JAG1)*	3.358865	0.030276	4.389256	0.000372	1.447692	0.329478
NM_002226	Jagged 2 *(JAG2)*	1.297184	0.264245	1.34398	0.062734	−1.01957	0.958371
NM_002228	Jun proto-oncogene *(JUN)*	**−1.40705**	0.027099	−1.52671	0.259297	−1.22093	0.564432
NM_032427	Mastermind-like 2 *(MAML2)*	2.191402	0.005553	2.132724	0.000279	1.070269	0.964675
NM_001200001	Notch-2 *(NOTCH2)*	47.35651	7.20E-05	59.36702	2.44E-06	2.488318	0.231699
NM_000435	Notch-3 *(NOTCH3)*	1.720812	0.006448	1.669143	0.00024	−1.00333	1.000000
NM_004557	Notch-4 *(NOTCH4)*	**−2.71993**	0.000887	−3.27107	0.000323	−1.69939	0.231699
NM_005378	V-myc myelocytomatosis viral related oncogene *(MYCN)*	**−1.27879**	0.026751	−1.21634	0.017491	−1.18255	0.677238
Oxidative Stress Response							
NM_001719	Bone morphogenetic protein 7 *(BMP7)*	15.579	0.0012	12.9433	1.17E-06	1.6101	0.2891
NM_000088	Collagen type 1, alpha 1 *(COL1A1)*	5.200	0.0018	4.8706	0.0001	1.2563	0.5705
NM_005794	Dehydrogenase/reductase (SDR family) member 2 *(DHRS2)*	19.624	0.0001	17.1225	1.42E-05	1.7535	0.2700
NM_005235	V-erb-a erythroblastic leukemia viral oncogene homolog 4 *(ERBB4)*	21.800	0.0002	19.8785	7.85E-07	2.3799	0.2502
NM_002084	Glutathione peroxidase 3 (plasma) *(GPX3)*	16.642	0.0003	16.9895	2.13E-06	1.6247	0.3183
NM_001008397	Glutathione peroxidase 8 (putative) *(GPX8)*	5.060	0.0029	4.5064	0.0001	1.2477	0.5761
NM_0021333	Heme oxygenase (decycling) 1 *(HMOX1)*	11.232	7.56E-05	9.145	3.14E-05	1.4662	0.4852
NM_005931	MHC class I polypeptide-related sequence B *(MICB)*	71.874	6.14E-05	81.096	2.62E-07	2.7817	0.2316
NM_004994	Matrix metallopeptidase 9 (gelatinase B, 92kDa gelatinase, 92kDa type IV collagenase) *(MMP9)*	5.252	0.00202	5.198	0.0238	1.2637	0.4267
NM_024420	Phospholipase A2, group IVA (cytosolic, calcium-dependent) *(PLA2G4A)*	7.690	0.00081	6.700	0.0110	1.2909	0.4072
NM_000962	Prostaglandin-endoperoxide synthase 1 (prostaglandin G/H synthase and	12.968	0.00016	9.145	3.14E-05	1.4691	0.2814

		PBmC		PmC		BmC	
Accn #	**Gene Title/Gene Symbol**	**F.C.**	**P-value**	**F.C.**	**P-value**	**F.C.**	**P-value**
	cyclooxygenase) *(PTGS1)*						
NM_000345	Synuclein, alpha (non A4 component of amyloid precursor) *(SNCA)*	4.230	0.0023	4.111	3.60E-05	1.2162	0.5611
NM_001178040	Syntaxin 3 *(STX3)*	20.771	9.76E-05	17.330	5.61E-06	1.8778	0.2998
Apoptosis and TNFR							
NM_001165	Baculoviral IAP repeat containing 3 *(BIRC3)*	6.5821	0.000693	6.758683	0.00138	1.4916	0.242024
NM_001226	Caspase 6, apoptosis-related cysteine peptidase *(CASP6)*	3.4102	0.00104	3.208055	0.000162	1.1764	0.739085
NM_015675	Growth arrest and DNA-damage-inducible, beta *(GADD45B)*	5.5125	0.002736	5.482137	2.35E-05	1.3944	0.391091
NM_000177	Gelsolin *(GSN)*	5.3800	0.001	5.109392	1.85E-05	1.5512	0.264134
NM_0021333	Heme oxygenase (decycling) 1 *(HMOX1)*	11.2322	7.56E-05	11.45708	5.12E-07	1.7320	0.277403
NM_000594	Tumor necrosis factor *(TNF)*	7.3495	0.000347	6.408024	8.56E-06	1.8115	0.231699
NM_001270507	Tumor necrosis factor, alpha-induced protein 3 *(TNFAIP3)*	2.2634	0.005704	2.187222	0.000655	1.4447	0.606515
NM_016639	Tumor necrosis factor receptor superfamily, member 12A *(TNFRSF12A)*	2.0183	0.007093	1.971959	0.014324	1.3393	0.410985
NM_001164155	Tumor necrosis factor receptor superfamily, member 19 *(TNFRSF19)*	6.1248	0.000168	6.084076	9.62E-07	1.6015	0.295686
NM_001145645	Tumor necrosis factor (ligand) superfamily, member 13b *(TNFSF13B)*	2.2388	0.003709	1.999324	0.00064	1.4443	0.299862
Cell Cycle Related							
NM_001759	G1/S specific cyclin D2 *(CCND2)*	87.4966	0.000182	95.4013	7.85E-07	1.8244	0.27847
NM_001258	Cyclin-dependent kinase-3 *(CDK3)*	**−1.9674**	0.002626	−1.5957	0.036293	−1.3050	0.354757
NF-kB Related							
NM_001165412	Nuclear factor of kappa light polypeptide gene enhancer in B-cells 1 *(NFKB1)*	**−1.2877**	0.165361	−1.1939	0.130896	−1.1483	0.612514
NM_025107	Homo sapiens myc target 1 (*MYCT1*)	2.0335	0.009183	2.2886	0.000631	1.6837	0.297559
NM_000600	Homo sapiens interleukin 6 (interferon, beta 2) (*IL6*)	**−1.3102**	0.056794	−1.3336	0.037262	−1.2640	0.382162
NM_001042533	MYC induced nuclear antigen (*MINA*)	1.8988	0.015987	1.4745	0.005057	1.6331	0.296344

[1] Treatment conditions include PCI-24781 and bortezomib minus control (PBmC), PCI-24781 minus control (PmC), and bortezomib minus control (BmC). Fold changes (f.c.) indicate sign fold changes, and p values (p) represent adjusted p values.